Solar Soft X-Ray Irradiance Variability, II: Temperature Variations of Coronal X-Ray Features

H. Adithya, Rangaiah Kariyappa, Kanya Kusano, Satoshi Masuda, Shinsuke Imada, Joe Zender, Luc Damé, Hegde Manjunath, Edward Deluca, Mark Weber

Solar Soft X-ray Irradiance Variability, II: Temperature Variations of Coronal X-ray Features

H. N. Adithya
Scikraft Education and Engineering Design Pvt. Ltd
Rangaiah Kariyappa (kari.hemi@gmail.com)
Indian Institute of Astrophysics
Kanya Kusano
Nagoya University
Satoshi Masuda
Nagoya University
Shinsuke Imada
The University of Tokyo
Joe Zender
European Space Research and Technology Center (ESTEC)
Luc Damé
LATMOS (Laboratoire Atmosphères
Edward DeLuca
Harvard-Smithsonian Center for Astrophysics
Mark Weber
Harvard-Smithsonian Center for Astrophysics

Research Article

Keywords: Sun: X-ray radiation, Sun: corona, Sun: coronal features, Sun: temperature of coronal features

Posted Date: June 29th, 2022

DOI: https://doi.org/10.21203/rs.3.rs-1778393/v1

Solar Soft X-ray Irradiance Variability, II: Temperature Variations of Coronal X-ray Features

H.N. Adithya[1,2] · Rangaiah Kariyappa[3,2]●● · Kanya Kusano[2] · Satoshi Masuda[2] · Shinsuke Imada[4] · Joe Zender[5] · Luc Damé[6] · Edward DeLuca[7] · Mark Weber[7]

Received Mmm DD, YYYY; accepted Mmm DD, YYYY

Abstract

Corona is the outermost layer of the Sun, which extends to several thousand kilometers from the visible photosphere. It is made up of very tenuous plasma but is very hot. The sudden increase of temperature in the coronal layer from the underlying chromosphere and photosphere makes it very interesting. The average temperature of a corona is measured about 2 MK, and it may show a large variation in temperature with respect to different surface features. Studying the variation of the temperature of the full-disk corona and of individual feature's

✉ R. Kariyappa
rkari@iiap.res.in

H.N. Adithya
adithyabhattsringeri@gmail.com

[1] Scikraft Education and Engineering Design Pvt. Ltd., Bangalore 560085, India

[3] Indian Institute of Astrophysics, Bangalore 560034, India

[2] Institute for Space-Earth Environmental Research (ISEE), Nagoya University, Nagoya, Japan

[4] Department of Earth and Planetary Science, The University of Tokyo, Tokyo 113-0033, Japan

[5] European Space Research and Technology Center (ESTEC), 2200 AG Noordwijk, The Netherlands

[6] LATMOS (Laboratoire Atmosphères, Milieux, Observations Spatiales),11 boulevard d'Alembert, 78280 Guyancourt, France

[7] Harvard-Smithsonian Center for Astrophysics, 60 Garden Street, Cambridge, MA, USA

temperature along with the solar cycle will be interesting and important to understand the Physics of the Sun.
Although an attempt has been made earlier to measure the temperature of coronal XBPs for a short period with high cadence of observations in localized regions, but the variation in temperature of the full-disk image and of individual features over the solar cycle is not measured yet. Since Hinode/XRT allows capturing images of the Sun in 8 different filters, it has got a unique feature that, using 2 different filters, the temperature map of the Sun can be generated. In order to study the temperature variations, we have used Al_mesh and Ti_poly filters of full-disk composite, level-2, X-ray images of the Sun obtained from Hinode/XRT. We developed a sophisticated python algorithm to segment different coronal features (ARs, CHs, BGs, & XBPs), derived the integrated intensity of all the features in both the filters, and generated the temperature maps of the corona using the filter ratio method. Because of the XRT straylight issue and unavailability of a good pair of images we have restricted our analysis for the period of 4 years (February 01, 2008 - May 08, 2012, covering the starting part of the solar cycle 24).
In this paper, *the first analysis* in using direct energy values of the coronal features from segmented solar disk and its relation to solar activity is presented. We have discussed the variations of the temperature of a full-disk corona, and of all the features (ARs, CHs, BGs & XBPs). We found from the time series plots of the average temperature of the full-disk and of all the features show temperature fluctuations and they vary in phase with the sunspot numbers (solar activity). Although the temperature of all the features varies but the mean temperature estimated for the whole observed period of the full-disk is around 1.39 $\pm$ 0.28 MK and active regions (ARs) will be around 1.98 $\pm$ 0.44 MK, whereas BGs, CHs & XBPs are 1.37 $\pm$ 0.26 MK, 1.34 $\pm$ 0.33 MK, and 1.52$\pm$ 0.34 MK respectively. In addition, we found that the mean temperature contribution estimated of the background regions (BG) will be around 91 %, whereas ARs, CHs, & XBPs are 5 %, 2 % and 2 % respectively to the average coronal temperature of the full-disk for the period: 2008-2012. The temperature values and their variations of all the features suggest that the features show a high variability in their temperature and that the heating rate of the emission features may be highly variable on solar cycle timescales. It is clear from the analysis that the filter ratio method can be directly used for temperature analysis of coronal features and to study their surface temperature variability as a function of solar magnetic activity.

Keywords: Sun: X-ray radiation – Sun: corona – Sun: coronal features – Sun: temperature of coronal features

1. Introduction

The solar corona is one of the interesting layers when it comes to the temperature variability of the Sun, a sudden spike up in temperature is still unsolved problem in Solar Physics. The average temperature of the corona measured about 1-2MK. Features of the corona such as active regions (ARs), coronal holes (CHs), the

background regions (BGs), and the X-ray bright points (XBPs) are dynamic in nature, their variability in temperature may directly affects the average temperature of the corona. Recently there was an attempt by (Kariyappa et al., 2011) in measuring the temperature of the XBPs observed by Hinode/XRT using filter ratio method (Ti_poly/Al_mesh) and they found that the XBPs show a high variability in their temperature and that the average temperature ranges from 1.1 MK to 3.4 MK. The variations in temperature are often correlated with changes in average X-ray emission. It is evident from the results of time series that the XBPs heating rate can be highly variable on short timescales, suggesting that it has a reconnection origin. But the variation in temperature of the full-disk and of individual features over the solar cycle is not yet measured and studied. It is a fundamental importance to measure the temperature structure of the solar corona and its features. The temperature of individual features is important to understand their contribution to total temperature of the corona. The filter ratio method has been used by (Weber et al., 2005) to show that the constant TRACE 195 A° /173 A° ratios can be reproduced by multithermal differential emission measures (DEMs) along the line of sight over a wide range of peak temperatures, in the limit of flat (i.e., very multithermal) DEMs, the filter ratio method is biased toward the ratio of the integrals of the temperature response functions. The temperature of a bright loop in an active region has been measured using a filter ratio method by (Hara et al., 1992), which indicates the existence of high temperature plasmas in the active region. The coronal temperatures have been determined from electron density profiles inferred from white light brightness measurements of the corona during solar eclipses (Lemaire, 2011).

Some studies have been done earlier to estimate the contribution of various coronal features to EUV & UV irradiance using spatially resolved observations (Kumara et al., 2014; Zender et al., 2017). In addition they investigated and discussed in detail the role of magnetic field on EUV & UV irradiance variability by comparing SWAP and AIA images with SDO/HMI magnetograms. Recently (Adithya et al., 2021), Paper I hereafter, have segmented the soft X - ray images obtained by Hinode/XRT for the period 2007 to 2020 and studied the total intensity of individual features and their contribution full-disk intensity values. The segmentation maps of the individual features observed with two filters will be used to derive the temperature maps by filter ratio method.

In this paper, we made an attempt *for the first time,* to use a direct energy values of the segmented solar disk and the segmented intensity maps of the two filters (Al_mesh & Ti_poly) to derive the corresponding temperature maps and then taken the filter ratio. The temperature of the segmented features such as active regions (ARs), coronal holes (CHs), background regions (BGs), and X-ray Bright Points (XBPs) are derived. In the following sections the details of the observations, analysis, results of temperature and contribution of ARs, CHs, BGs, XBPs, and full-disk intensity (FDI) are presented and discussed.

2. Observations and analysis

To study the temperature variation of the solar corona, we used full-disk daily images taken by the X-Ray Telescope onboard the Hinode mission (Hinode/XRT).

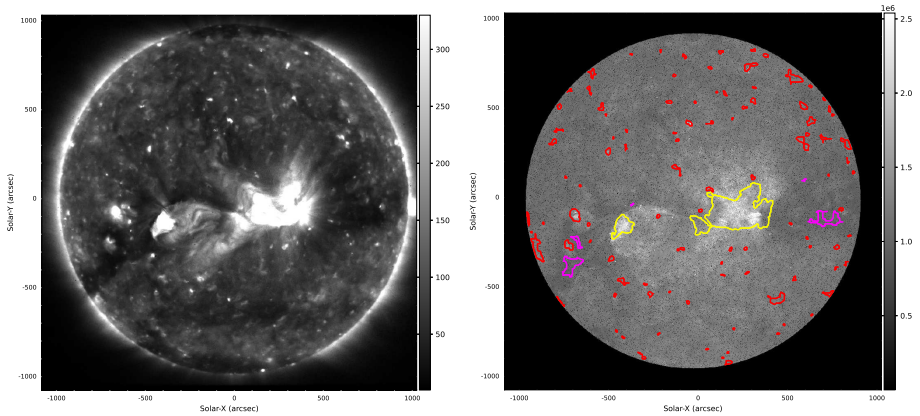

Figure 1. A sample of a composite image (*left panel*) and temperature map (*right panel*) showing all the features (ARs, CHs, BGs and XBPs) obtained from Hinode/XRT on February 04, 2008.

The details on the design, calibration and measured performance of the XRT instrument up to the focal plane and the CCD camera and data handling are discussed in (Kosugi et al., 2007; Golub et al., 2007). The level-2 data from February 1, 2008 to May 8, 2012 was downloaded from http://solar.physics .montana.edu/HINODE/XRT/SCIA/synop_images/syncmp_FITS. For this data, the xrt_prep procedure has been applied already. Which subtracts a dark frame, and carries out the vignetting correction, the removal of high-frequency noise, and the normalisation by exposure time. In addition, the quality of the archived full-disk images has been further improved with the following three methods: (i) Images are composites of long+short exposure images to provide extended dynamic ranges and to eliminate saturations, (ii) small contamination of spots on the CCD have been corrected in the images by replacing affected pixels with the averaged intensity of the surrounding area, and (iii) the pointing information has been updated with a recently developed database that co-aligns XRT with other solar instruments (Takeda, Yoshimura, and Saar, 2016). The XRT data set used in this analysis contains composite images. It is difficult for XRT to take a single image that sees both faint and bright features, hence the composite synoptic data sets include both long and short exposure images to observe both faint and bright features. Therefore, the composite image can represent a greater dynamic range than the instrument itself is capable of producing in a single image and the composite images were suitable to use for this analysis of all the features.

In our paper I, we segmented the coronal features such as Active regions (ARs), Coronal holes (CHs), Background (BG), X-ray Bright points (XBPs) and studied the intensity variation of both full-disk and individual features for the period February 2007- March 2020. Paper II is the continued work of paper I and in this paper we are focusing on the temperature variation of full-disk and of individual features.

XRT has eight diagnostic filters, based on the availability of good images we selected Ti_poly and Al_mesh filters for detailed analysis. Since these two thin

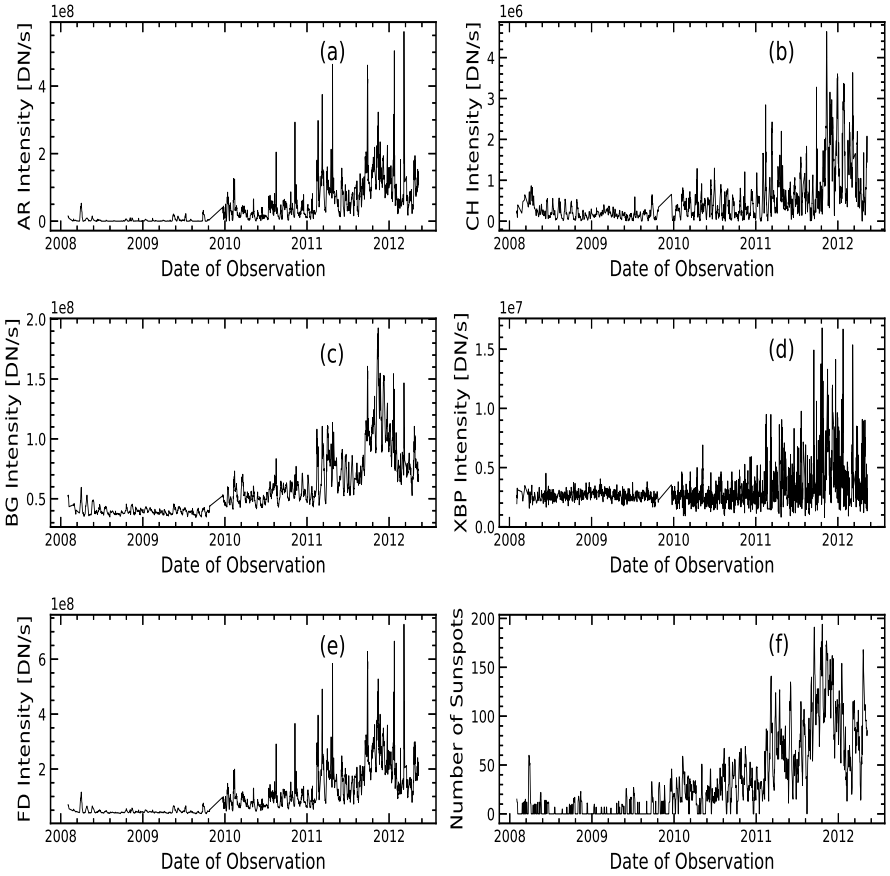

Figure 2. Total intensity of solar X-ray features: (a) ARs, (b) CHs, (c) BGs, (d) XBPs, (e) full-disk intensity (FDI) (observed from Hinode/XRT in Al_mesh filter), and for comparison with (f) sunspot numbers (SSN) for a period starting from February 01, 2008 to May 08, 2012

filters are most frequently and regularly taken, they also provide high signal-to-noise ratio images over the solar activity. We had to restrict our analysis only for 4 years because the Ti-poly filter was affected by the XRT stray light event on 9th May 2012 and onwards.

Off-centered and low signal to noise ratio images are manually removed from the data set. Because of XRT OP heater issue there are no images available in Al_mesh and Ti_poly filters for the period October October 23, 2009 to December 19, 2009. The data set considered for the analysis has images of sizes 1024x1024 and 2048x2048 pixels for the period from February 01, 2008 to May 08, 2012.

Number of 1024x1024 pixels size image pairs(Ti_poly and Al_mesh)=1884

Number of 2048x2018 pixels size image pairs=132

Total number of image pairs=2016

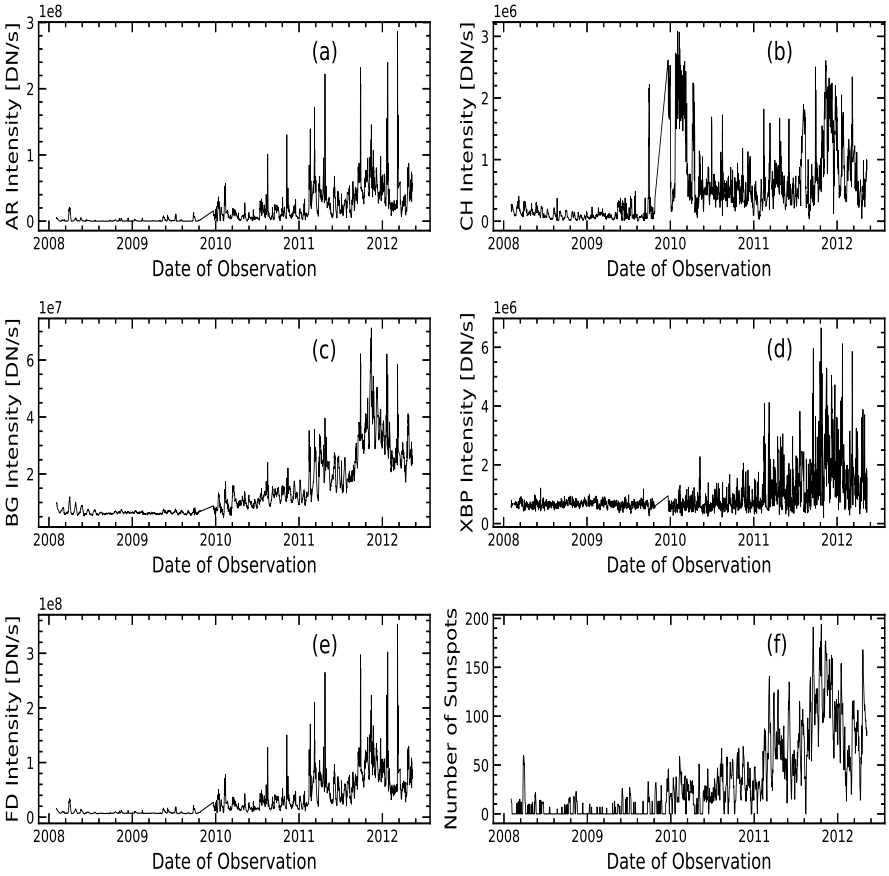

.

Figure 3. Total intensity of solar X-ray features: (a) ARs, (b) CHs, (c) BGs, (d) XBPs, (e) full-disk intensity (FDI) and (f) SSN, observed from Hinode/XRT in Ti_poly filter for a period starting from February 01, 2008 to May 08, 2012

We used the filter ratio method (Narukage et al., 2011, 2014) to calculate the temperature of each pixel in the image. The filter ratio method assumes that the corona is isothermal. According to the filter ratio method using the ratio of two filter's response functions and the corresponding filter's intensity ratio, the temperature of the corona can be calculated. The response of the filters with respect to temperature varies over time because of CCD contamination. In order to reduce CCD contamination, a CCD bakeout is done regularly (Takeda, Yoshimura, and Saar, 2016).

The response function of the two filters for each image with respect to the thickness of contamination layer was extracted using 'make_xrt_temp_resp.pro' in IDL/SSW routine. We have developed a sophisticated python algorithm to generate temperature maps from Ti_poly and Al_mesh images along with their

response function. And we have used the segmentation maps generated in our previous study (Paper I) to extract the average temperature of X-ray features.

The flow chart of the algorithm to derive the temperature values is as follows:

1. The segmentation map is generated by segmenting the Al_mesh image as described in our paper I and the full-disk intensity of the image is calculated.

2. Almost the same time of observation, a Ti_poly image (having a max 2-3 min time difference in observation) is taken and full-disk(FD) intensity is calculated.

3. The intensity ratio map was generated by co-aligning disk centres of both the images and dividing the Ti_poly image with the Al_mesh image.

4. Responses of both the filters for the range of (or different) temperature are generated using SSW routines make_xrt_wave_resp.pro & make_xrt_temp_resp.pro for each image corresponding to time of observation.

5. The ratio of Ti_poly filter/Al_mesh filter responses vs temperature plot is generated.

6. Since the ratio of filter responses is equal to the ratio of intensities,

F1/F2=I1/I2, where F1=Filter response of Ti_Poly, F2=Filter response of Al_mesh, I1=Intensity of Ti_poly image,I2=Intensity of Al_mesh image,

the temperature map is generated by mapping intensity ratio values to corresponding temperature values by referring to the ratio of the filter's response curve vs the temperature plot.

7. The segmentation map is overlaid on the temperature map and the average temperatures of FD, ARs, CHs, BGs, and XBPs are extracted from the temperature map. A sample of a composite image (left panel) and temperature map (right panel) showing all the features (ARs, CHs, BGs and XBPs) obtained from Hinode/XRT on February 04, 2008 is shown in Fig.1.

The time series of the temperature of FD, ARs, CHs, BGs and XBPs have been generated and compared with SSN, sunspot numbers. The important results of the temperature analysis are presented and discussed in the following section.

3. Results and discussion

Using our algorithm, presented in the previous Paper I, we segmented coronal X-ray features automatically from full-disk Hinode/XRT images observed in Al_mesh filter for the period from February 14, 2007 to March 31, 2020, which covers Solar Cycle 24 and discussed the important results of their intensity and area variations. We derived the corresponding total intensity, area (total number of pixels) and contribution of ARs/CHs/BGs/XBPs. We have compared the total intensity and area of ARs/CHs/BGs/XBPs to full-disk total X-ray intensity (FDI) and derived their contribution to FDI and GOES (1 – 8 Å) X-ray flux for each day for the whole period. We observed from the time series plots of ARs/CHs/BGs/XBPs/FDI taken with Al_mesh in comparison with GOES and

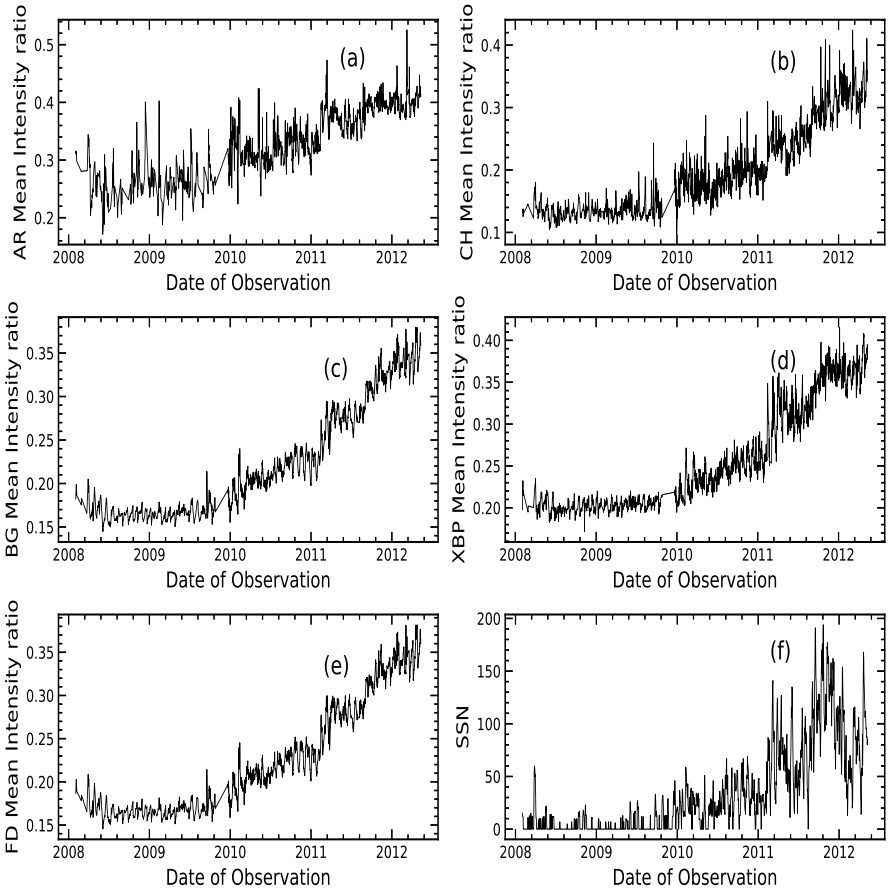

Figure 4. Variation in the intensity ratios (Ti_poly/Al_mesh) of all the features: (a) ARs, (b) CHs, (c) BGs, (d) XBPs, (e) FDI & (f) SSN for the period from 2008 to 2012

sunspot numbers that the intensity of all the features is well correlated with FDI, GOES total X-ray flux and sunspot numbers. This indicates that the long-term variability of segmented features and full-disk intensity shows a correlation with GOES (1 – 8 Å) solar X-ray flux and the sunspot numbers, this implies that the changes are in phase with the solar cycle.

In this paper, we have analysed the images observed in Al_mesh and Ti_poly filters for the period: February 2008 - May 2012 and derived the segmentation maps and the temperature maps from the filters ratios (Ti_poly/Al_mesh) and then the segmentation maps will be overlying on temperature maps, to estimate the average temperature of all the features. The first analysis in using the direct energy values of the segmented features to derive the temperature values is presented in detail. The variations of temperature of all the coronal features and full-disk are discussed in the following section.

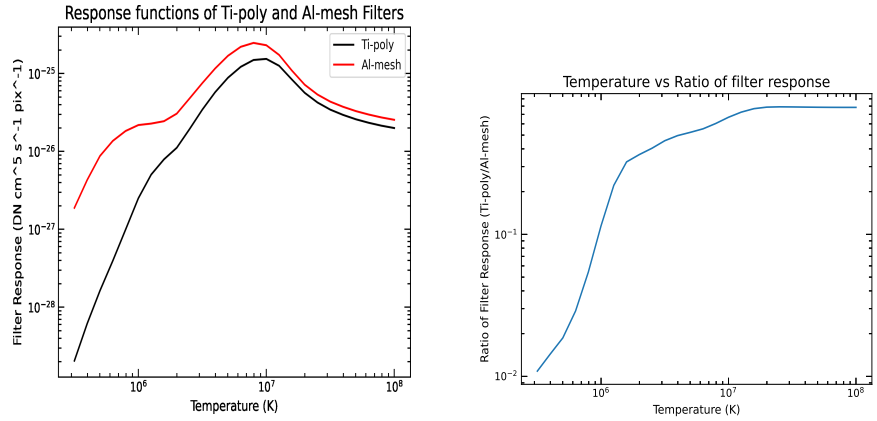

Figure 5. Variations in the XRT Ti_poly & Al_mesh filter responses as a function of temperature after including the contamination layer (left panel) and filter ratio response as a function of temperature (right panel), which corresponds to Fig.1 image (February 04, 2008)

The time series of integrated intensity of each of the coronal features and full-disk intensity for the Hinode/XRT X-ray images observed in Al_mesh & Ti_poly filters and sunspot numbers (SSN) are shown in Figs. 2 and 3. The intensity of all the features vary with the phase of the solar cycle. It is also clear from Figs. 2 & 3 that on an average over the solar cycle the integrated intensity of BGs is larger than the integrated intensity of ARs, CHs, and XBPs, but the contribution of ARs will become more dominant around solar maximum. Note that the BG intensity values will be slightly contaminated by the fuzzy regions (brighter than BG & less than ARs, as seen in Fig.1) present around the ARs while segmenting the features. However, this does not change the results and conclusions. We also noticed that there is good correlation between the intensity of all the features in comparison with sunspot numbers indicating that they vary with solar activity.

From the time series shown in Figs.(2) and (3), we noticed that the integrated intensity values of all the features exhibit the expected 27 day modulation due to the solar rotation, similar to sunspots at the photospheric level. The observed intensity variation is due to the change of feature's intensity and due to the expansion/shrinkage of the area of the features during their evolution. This suggests that the intensity and area of the coronal features have to be taken into account in the models to explain the irradiance variations.

Figs. 2 and 3 are the result of two effects: an actual increase in the surface brightness of the features and an increase in the area of the features. The latter effect can be mitigated by taking the ratio of images observed in two filters. We derived the ratio of the intensity values of each feature observed with two filters. The variations of the intensity ratios are presented in Fig. 4 for all the features. It is evident from these figures that the fluctuations in the intensity ratio of the features are similar to the intensity oscillations shown in Figs. 2 and

Table 1. Spearman rank correlation coefficients between Sunspot numbers (SSN) and the average temperature of coronal features (ARs, CHs, BGs and XBPs) & FDI as observed on Hinode/XRT

	Correlation Coefficients (R)
ARs vs SSN	0.82
CHs vs SSN	0.82
BGs vs SSN	0.86
XBPs vs SSN	0.87
FDI vs SSN	0.87

3. In Fig.4, we have plotted the intensity ratios of the filters Ti_poly & Al_mesh and used them to make the plots of temperature response curves presented in Fig.5 (left panel). The Fig.5 represents the filter respenses as a function of temperature for both the filters (Ti_poly & Al_mesh). These curves have been used to derive the temperature of individual features and full-disk for the entire period. To determine the temperature of the features, we derived the XRT filter temperature response curves for Ti_poly and Al_mesh after considering the contamination layer thickness (see Fig. 5). The ratio of filter response as a function of temperature, for the image (observed on Febrary 04, 2008) shown in Fig.1, is plotted in Fig.5 (right panel). Using these filter temperature response curves and the intensity ratios, we determined the temperature of each feature. We estimated the errors in the temperatures by assuming photon statistics for the filter fluxes, and folding these through the filter ratio versus temperature to estimate temperature errors. We stress that these are random errors only; systematic errors due to uncertainties in, e.g., calibrations, the contamination layer, etc. are not included, but are smaller than the random errors. In Fig. 6 we show the temporal variations in average temperature of all the features, the full-disk and compared with sunspot numbers. The average temperature of the full-disk and of all the features show temperature fluctuations and they vary with the sunspot numbers (solar activity). It is clear that the temperature is minimum during 2008 and 2009 and slowly started raising during interphase period. Although the temperature of all the features varies but the mean temperature estimated for the whole observed period of the full-disk is around 1.39 $\pm$ 0.28 MK and active regions (ARs) will be around 1.98 $\pm$ 0.44MK, whereas BGs, CHs & XBPs are 1.37 $\pm$ 0.26 MK, 1.34$\pm$ 0.33 MK, and 1.52 $\pm$ 0.34 MK respectively. We noticed that the temperature of XBPs is greater than the temperature of BGs and CHs. That means the XBPs are more intense magnetic regions, which may contribute to total surface temperature. It has been observed and reported earlier that the XBPs show a high variability in their temperature and that the average temperature ranges from 1.1 MK to 3.4 MK (Kariyappa et al., 2011).

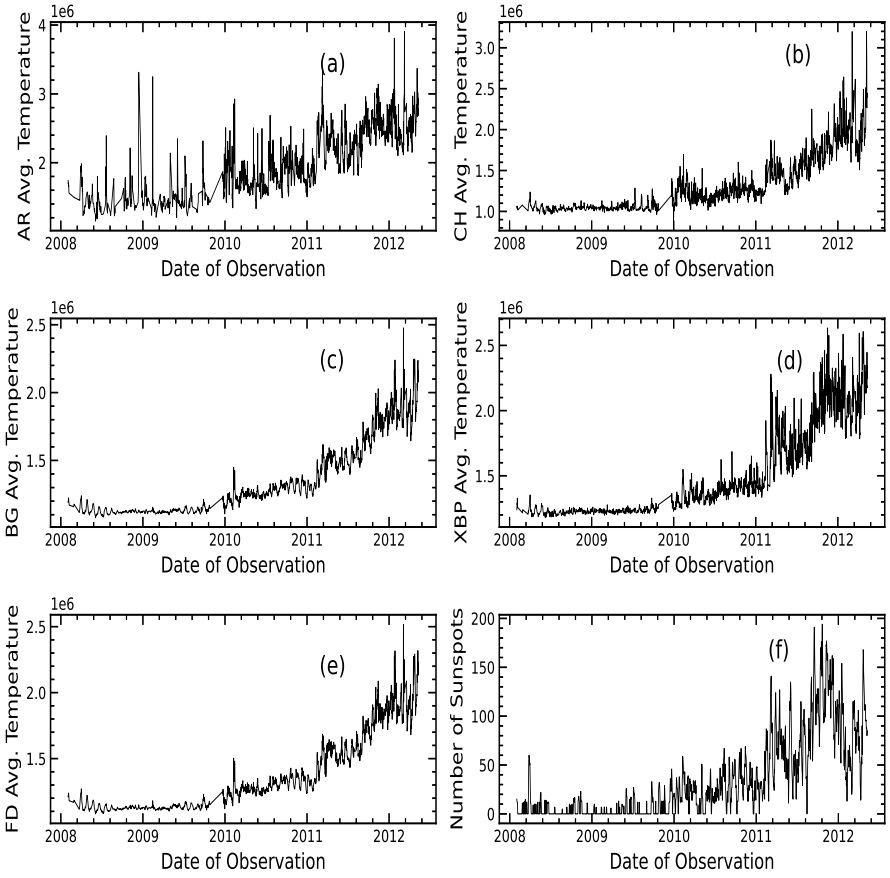

Figure 6. Average temperature of solar X-ray features derived from filter ratio method: (a) ARs, (b) CHs, (c) BGs, (d) XBPs, (e) Full-disk temperature (FDT) and (f) SSN, observed from Hinode/XRT for a period starting from February 01, 2008 to May 08, 2012

Considering the high temperature and a large number of XBPs present over the full-disk at any time, the XBPs contribute significantly to total intensity (Adithya et al., 2021) and temperature variability of the full-disk and to the heating of the corona at the sites of XBPs. The temperature values and their variations of all the features suggest that the features show a high variability in their temperature and that the heating rate of the emission features may be highly variable on solar cycle timescales. The evoloution of these features would require a detailed study of thermal and magnetic properties of the features.

In Fig. 7, we have plotted the average temperature of all the features (ARs, CHs, BGs & XBPs) and the full-disk temperature (FD) versus the sunspot numbers for a period February 2008 to May 2012. We have determined the Spearman rank correlation coefficients of the segmented features with the sunspot number values and their correlation coefficients (R) are presented in Table 1. As seen from

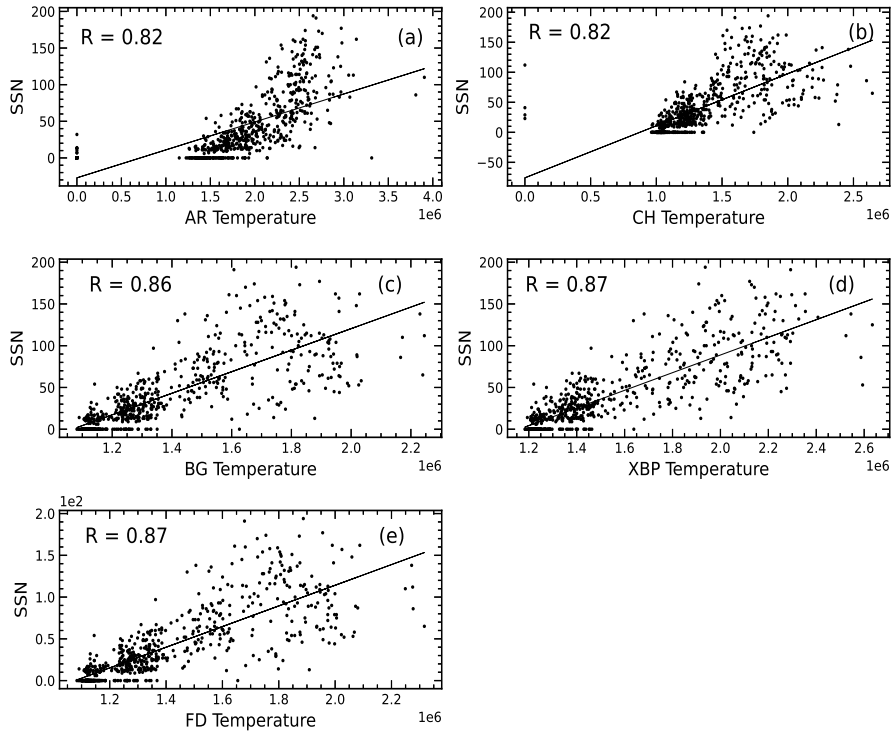

Figure 7. Average temperature of all the features: (a) ARs, (b) CHs, (c) BGs, (d) XBPs,& (e) FDT are ploted versus SSN for the period starting from February 01, 2008 to May 08, 2012

the scatter plots (Fig. 7) and the results of the correlation coefficients (in Table 1), the average temperature of all the features are well correlated with sunspot numbers. We can conclude that the spatially resolved images are important asset to use to understand the integrated intensity and average temperature variabilities of the Sun when we observe the Sun as a Star (true also in the case of solar type stars, if they have stellar X-ray irradiance measurements simultaneously in any two filters, where we can use Sun as a calibrator).

Since the full-disk temperature (FDT) values have been measured Sun as a star, they do not reveal directly the individual contribution of different features. In order to determine the contribution of the segmented X-ray features to FD temperature, we used an expression:

Temperature Contribution (TC in %) = (100 × FT) / FDT, where FT is feature's temperature integrated over its area and FDT is full-disk temperature.

Figure 8 represents the variation in the contribution of temperature of all the X-ray coronal features (ARs, CHs, BGs and XBPs) to full-disk temperature variations. We noticed in Figure 8(a) and Figure 8(b) that the contribution of ARs and CHs changes with the phase of the solar cycle, whereas the BGs and XBPs temperature contribution values, presented in Figure 8(c) and Figure

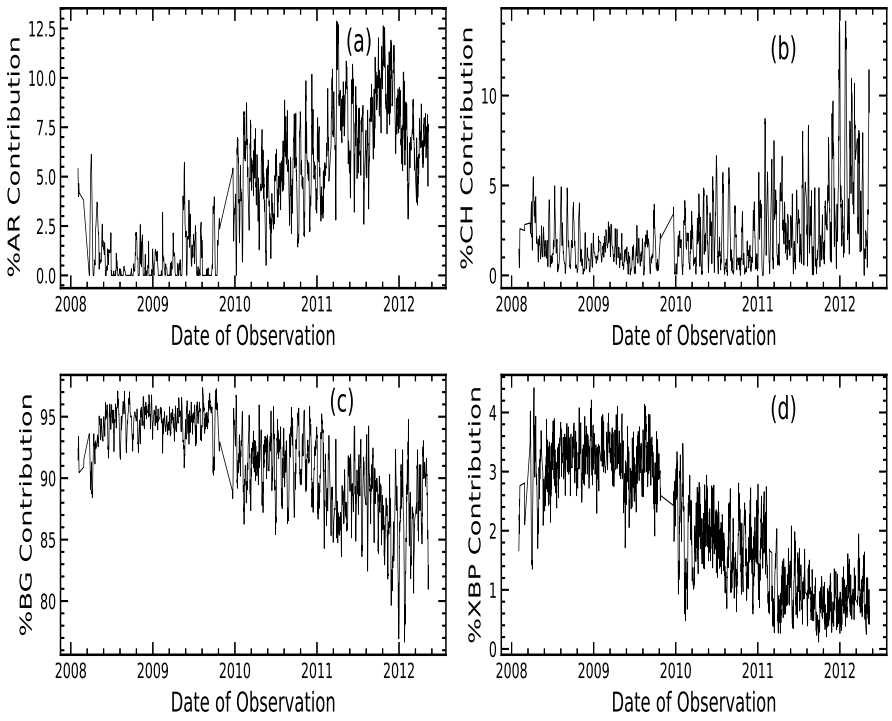

Figure 8. Variation of temperature Contribution of (a) ARs, (b) CHs, (c) BGs and (d) XBPs to full-disk temperature (FDT), for a period starting from February 01, 2008 to May 08, 2012

8(d), respectively, are inversely proportional to solar activity (large contribution during solar minimum and smaller during a solar maximum period). We also observed a similar behavior or pattern between the variations of the area (not presented here) and percentage of temperature contributions (plotted in Figure 8) of all the coronal features, showing ARs and CHs vary in phase with the solar activity and whereas the BGs and XBPs are anti-correlated. We found that the mean temperature contribution estimated of the background regions (BGs) will be around 91 %, whereas ARss, CHs, & XBPs are 5 %, 2 % and 2 % respectively to the average coronal temperature of the full-disk for the period: 2008-2012. Usually the ARs are more intense, magnetic and brighter regions than other features, but they are contributing less to the total surface temperature of the corona, because the ARs will be covered by less area over the full-disk compared to BG regions. Whereas the BG regions are contributing dominantly (about 91 %), simply because of the large filling factor (large area) over the disk. Since the brightness, temperature and area of the features are changing and are highly variable and hence they will have more influence in the variation of total temperature.

The segmented coronal X-ray features observed in X-ray wavelength and their intensity and temperature maps can be used as proxies to isolate the underlying corresponding photospheric magnetic structures for further studies. A similar studies have been done for UV emission features in relation to photospheric magnetic elements (Zender et al., 2017). In our future work we plan to apply our algorithm capabilities to overlay the XRT full-disk segmented images/maps on to SOHO/MDI and SDO/HMI full-disk magnetograms and to segment the photospheric magnetic features corresponding to segmented coronal X-ray features. The extraction of magnetic field of all the features would help to understand the temperature variability and the role of magnetic field in the intense regions (for example XBPs). It is interesting to study the relation between the temperature of the coronal features and the strength of the magnetic field, and how the magnetic field plays a role in driving the different brightenings and different temperature values and in the heating mechanisms of the corona at the sites of all these features. Combining the results of the variation of intensity field, temperature field and megnetic field associated with the coronal features will lead better in understanding the atmosphere of the corona and its heating mechanism.

Acknowledgements Hinode is a Japanese mission developed and launched by ISAS/JAXA, in collaboration with NAOJ as a domestic partner, NASA and STFC (UK) as international partners. The Hinode science team at ISAS /JAXA has conducted the Scientific operation of the Hinode mission. This team mainly consists of scientists from different institutes in the partner countries. JAXA and NAOJ (Japan), STFC (U.K.), NASA (U.S.A.), ESA, and NSC (Norway) have provided the support for the post-launch operation. The Hinode team had contributed all their efforts in the design, build, and operation of the mission. RK wish to express his sincere thanks to all members of ISEE, Nagoya University for the support provided under the Programs of ISEE Joint International Research and Visiting Professorship. HNA had visited ISEE/Nagoya University for 3 months under the sponsership of SCOSTEP Visiting Scholar Program and the support of ISEE. Authors would like to thank Aki Takeda for her useful suggestions in using the XRT images.

References

Adithya, H.N., Kariyappa, R., Shinsuke, I., Kanya, K., Zender, J., Damé, L., Gabriel, G., DeLuca, E., Weber, M.: 2021, Solar Soft X-ray Irradiance Variability, I: Segmentation of Hinode/XRT Full-Disk Images and Comparison with GOES (1 - 8 Å) X-Ray Flux. *Solar Phys.* **296**, 71. DOI. ADS.

Golub, L., Deluca, E., Austin, G., Bookbinder, J., Caldwell, D., Cheimets, P., Cirtain, J., Cosmo, M., Reid, P., Sette, A., Weber, M., Sakao, T., Kano, R., Shibasaki, K., Hara, H., Tsuneta, S., Kumagai, K., Tamura, T., Shimojo, M., McCracken, J., Carpenter, J., Haight, H., Siler, R., Wright, E., Tucker, J., Rutledge, H., Barbera, M., Peres, G., Varisco, S.: 2007, The X-Ray Telescope (XRT) for the Hinode Mission. *Solar Phys.* **243**, 63. DOI. ADS.

Hara, H., Tsuneta, S., Lemen, J.R., Acton, L.W., McTiernan, J.M.: 1992, High-Temperature Plasmas in Active Regions Observed with the Soft X-Ray Telescope aboard YOHKOH. *Pub. Astron. Soc. Japan* **44**, L135. ADS.

Kariyappa, R., Deluca, E.E., Saar, S.H., Golub, L., Damé, L., Pevtsov, A.A., Varghese, B.A.: 2011, Temperature variability in X-ray bright points observed with Hinode/XRT. *Astron. Astrophys.* **526**, A78. DOI. ADS.

Kosugi, T., Matsuzaki, K., Sakao, T., Shimizu, T., Sone, Y., Tachikawa, S., Hashimoto, T., Minesugi, K., Ohnishi, A., Yamada, T., Tsuneta, S., Hara, H., Ichimoto, K., Suematsu, Y., Shimojo, M., Watanabe, T., Shimada, S., Davis, J.M., Hill, L.D., Owens, J.K., Title, A.M., Culhane, J.L., Harra, L.K., Doschek, G.A., Golub, L.: 2007, The Hinode (Solar-B) Mission: An Overview. *Solar Phys.* **243**, 3. DOI. ADS.

Kumara, S.T., Kariyappa, R., Zender, J.J., Giono, G., Delouille, V., Chitta, L.P., Damé, L., Hochedez, J.-F., Verbeeck, C., Mampaey, B., Doddamani, V.H.: 2014, Segmentation of coronal features to understand the solar EUV and UV irradiance variability. *Astron. Astrophys.* **561**, A9. DOI. ADS.

Lemaire, J.F.: 2011, Determination of coronal temperatures from electron density profiles. *arXiv e-prints*, arXiv:1112.3850. ADS.

Narukage, N., Sakao, T., Kano, R., Hara, H., Shimojo, M., Bando, T., Urayama, F., Deluca, E., Golub, L., Weber, M., Grigis, P., Cirtain, J., Tsuneta, S.: 2011, Coronal-Temperature-Diagnostic Capability of the Hinode/ X-Ray Telescope Based on Self-Consistent Calibration. *Solar Phys.* **269**, 169. DOI. ADS.

Narukage, N., Sakao, T., Kano, R., Shimojo, M., Winebarger, A., Weber, M., Reeves, K.K.: 2014, Coronal-Temperature-Diagnostic Capability of the Hinode/ X-Ray Telescope Based on Self-consistent Calibration. II. Calibration with On-Orbit Data. *Solar Phys.* **289**, 1029. DOI. ADS.

Takeda, A., Yoshimura, K., Saar, S.H.: 2016, The Hinode/XRT Full-Sun Image Corrections and the Improved Synoptic Composite Image Archive. *Solar Phys.* **291**, 317. DOI. ADS.

Weber, M.A., Schmelz, J.T., DeLuca, E.E., Roames, J.K.: 2005, Isothermal Bias of the "Filter Ratio" Method for Observations of Multithermal Plasma. *Astrophys. J. Lett.* **635**, L101. DOI. ADS.

Zender, J.J., Kariyappa, R., Giono, G., Bergmann, M., Delouille, V., Damé, L., Hochedez, J.-F., Kumara, S.T.: 2017, Segmentation of photospheric magnetic elements corresponding to coronal features to understand the EUV and UV irradiance variability. *Astron. Astrophys.* **605**, A41. DOI. ADS.